

STRUCTURAL, DIELECTRIC, FERROELECTRIC AND MAGNETIC PROPERTIES OF MN-DOPED BIFEO₃ NANOPARTICLES SYNTHESIZED BY SOL-GEL METHOD

Ghanshyam Arya, Ashwani Kumar, Mast Ram and Nainjeet Singh Negi
Department of Physics, Himachal Pradesh University, Shimla, India

ABSTRACT

BiFe_{1-x}Mn_xO₃ (x = 0.0–7.5%) nanoparticles were successfully synthesized by tartaric acid assisted sol-gel method followed by rapid cooling process. XRD patterns indicate secondary phases in pure BiFeO₃ (BFO) which get suppressed with Mn concentration up to 5%. The observation of absorption peaks at 559 cm⁻¹ and 432 cm⁻¹ in FTIR spectra confirms the formation perovskite structure. The Mn substitution at B-site of BFO improves the particles surface morphology and reduces the average particles size to around 65nm. Dielectric constant increases from 19 for pure BFO to 46 for 5% composition while their loss tangent decreases from 0.2 to 0.016, respectively. A small dielectric relaxation peak is observed for 2.5% composition which disappears for 5% due to reduction of charged defects such as oxygen ion vacancies. The ferroelectric behavior improves with Mn-doping and maximum remnant polarization value of 1.8μC/cm² at a maximum applied field of 80kV/cm is observed for 5% composition. Enhanced magnetic property is observed for different Mn contents with maximum value of saturation magnetization of 0.20emu/g at room temperature.

KEYWORDS: Nanomaterials; Dielectric properties; Magnetic properties; ferroelectric properties;

I. INTRODUCTION

Multiferroic materials possess potential applications in the field of materials science and are in active research owing to the presence of strong coupling of electric, magnetic and structural order parameters, which give rise to simultaneous occurrence of ferroelectricity, ferromagnetism and ferroelasticity [[1-4]. These materials show strong magnetoelectric coupling and hence can find application in information storage, spintronics, sensors and microelectronics devices. Among the well-studied multiferroic materials (YMnO₃, BiMnO₃, BiFeO₃ etc), bismuth ferrite (BiFeO₃) with rhombohedral distorted perovskite (ABO₃) structure has taken considerable attention on account of being a multiferroic materials at room temperature. It shows ferroelectricity with a high Curie temperature (T_C = 830⁰C) and G-type antiferromagnetism up to Neel temperature T_N=370⁰C [5]. Currently, bulk BFO is not suitable for application because of its high conductivity which arises mainly from charge fluctuation of Fe and antiferromagnetic behavior at room temperature which prohibits linear magnetoelectric effect [6, 7]. Therefore, many attempts have been made to the realization of enhanced multiferroic properties in nanostructure BFO where significant size effect on the improvement of magnetic properties was evidenced [8-12]. The substitution of various metal ions in BFO has already been carried out by many research groups and their relentless efforts have brought new height in the research area of BFO [13-20]. Among the transition metal ions, the doping of Mn at Fe site reduces leakage current density and improves magnetic behavior which is essential for real multiferroic materials.

Recently, an enhanced magnetic properties of Mn doped BFO nanoparticles prepared by hydrothermal method has been reported, but there is no report on detail investigation of Mn substituted BFO

nanoparticles prepared by rapid sintered sol-gel method [21]. In the present paper, we report a detail study of effect of Mn on structural, dielectric, magnetic and ferroelectric properties of Mn doped BiFeO₃ nanoparticles synthesized by rapid sintered sol-gel method. Interesting results are observed for particular composition (5%) of Mn which can be useful for application in many practical devices.

II. EXPERIMENTAL DETAILS

A sol-gel method was employed for synthesizing pure and Mn doped BFO nanoparticles. The appropriate amount of Bi(NO₃)₃·5H₂O, Mn(NO₃)₃·6H₂O, and Fe(NO₃)₃·9H₂O (compositions 0%, 2.5%, 5%, 7.5% of Mn) were first dissolved in 2-methoxyethanol. Tartaric acid in 1:1 molar ratio with respect to metal nitrates was added to the precursor solution. The gel of mixed solution was dried at 80°C. The resulting dry gel was grinded into powder followed by calcinations at 550°C for two hours. After that, the powders were sintered for 450 s in air at 820 °C, and then subsequently cooled rapidly to room temperature. After mixing PVA solution as binder with the well grinded powder, pallets of different samples were made by applying hydraulic pressure of about 10 tons. Well dense pallets were obtained after rapid sintering at 820°C for half an hour. For electrical characterization, both sides of the pallets were polished with silver paste to form two electrodes for conduction mechanism. The crystal structure of the samples was carried out by a Philips XPERT-PRO X-ray diffractometer using Cu K α radiation. Scanning electron microscopic (SEM) and Tunneling electronic microscopy analysis were performed to study the homogeneity and to determine the particle size. Dielectric measurements were carried out with Wayne Kerr, 65000B Precision Impedance Analyzer. Magnetic and ferroelectric measurements were performed with Vibratory Sample Magnetometer (VSM) and P-E Loop Tracer respectively. The variation of resistivity with Mn contents was measured with Keithley 2611 source meter.

III. RESULT AND DISCUSSION

The XRD patterns of pure and Mn-doped BFO nanoparticles are shown in figure 1. Observed X-ray diffraction peaks pattern of sintered powder could be indexed to distorted rhombohedral structure of BiFeO₃ with space group R3c [22]. It can be also noted from XRD pattern that the crystallites of samples increase with increasing Mn contents and also suppress the formation of impurity phases up to 5% composition.

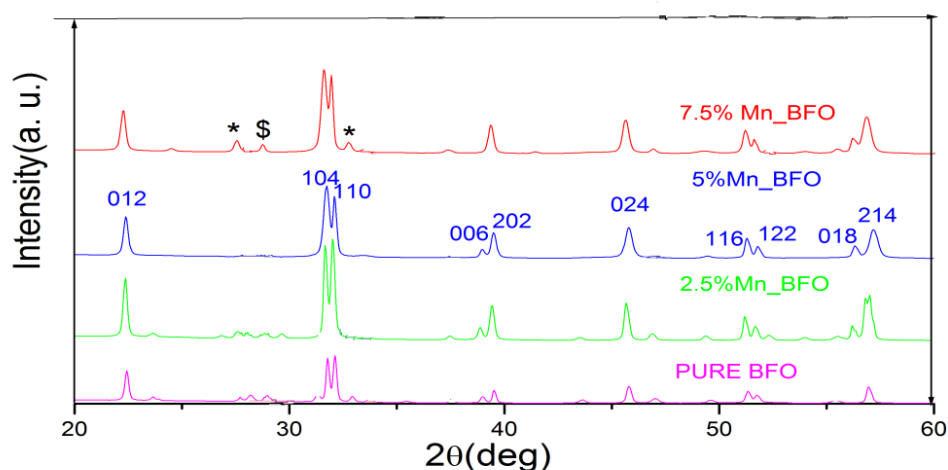


Fig.1. X-ray diffraction (XRD) patterns for BiFe_{1-x}Mn_xO₃ (0.0 ≤ x ≤ 0.075) nanoparticles

The impurity phases as observed in pure and 7.5% sample may be attributed to Bi₂Fe₄O₉ and Bi₄₆Fe₂O₇₂ which has also been reported by other author (23-24). The lattice parameters (equivalent hexagonal for x ≤ 0.075) of BiFe_{1-x}Mn_xO₃ are: for x=0.0, a=5.5748, c= 13.894, x=0.05, a=5.5439, c=13.921, x=0.075, a=5.5345, c=13.796. The calculated value of lattice parameters indicates that there is a continual change in lattice constant when Mn²⁺ ion is substituted for Fe³⁺ ion. The average

crystallite size as calculated from XRD pattern by applying Scherer equation are 98, 84, 72 and 65nm for 0%, 2.5, 5% and 7.5% composition of Mn, which indicates the nanostructure characteristics of these samples. The decrease in crystallite sizes and lattice parameters with increasing Mn contents is attributed to the smaller ionic radii of Mn^{2+} (0.46 Å) ion than that of Fe^{3+} (0.645 Å) ion which might inhibit the crystal growth.

The room temperature FTIR spectra for 5% doped sample is shown in figure 2. The strong absorption peaks near 558 cm^{-1} and another near 432 cm^{-1} are assigned to Fe–O stretching and bending vibration, respectively, being characteristics of the octahedral FeO_6 group in the perovskite compounds [25, 26].

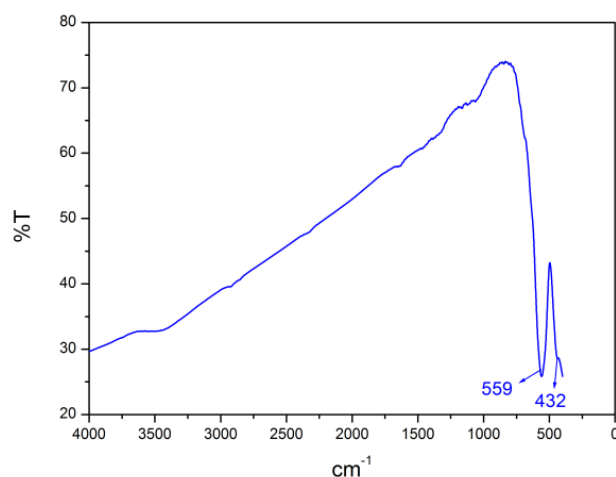


Fig.2. FTIR spectra of 5% Mn doped BFO nanoparticles

The formation of perovskite structure in our sample can be confirmed from the presence of metal oxide band at $400\text{--}600\text{ cm}^{-1}$ [27]. To further confirm the substitution of Mn at Fe-site, EDAX spectra of 5% Mn doped BFO was measured and shown in Figure 3(d). The EDAX image taken from the selected area of different grains confirms the presence of Bi, Fe and Mn elements. No extra impurities peaks arise from XRD graphs with Mn contents, which further support the fact that Mn has been successfully substituted in Fe site.

The surface morphologies of pure and Mn doped BFO nanoparticles have been studied from scanning electron microscopy (SEM). The SEM images of pure and 5% compositions are shown in figures 3(a) and (b).

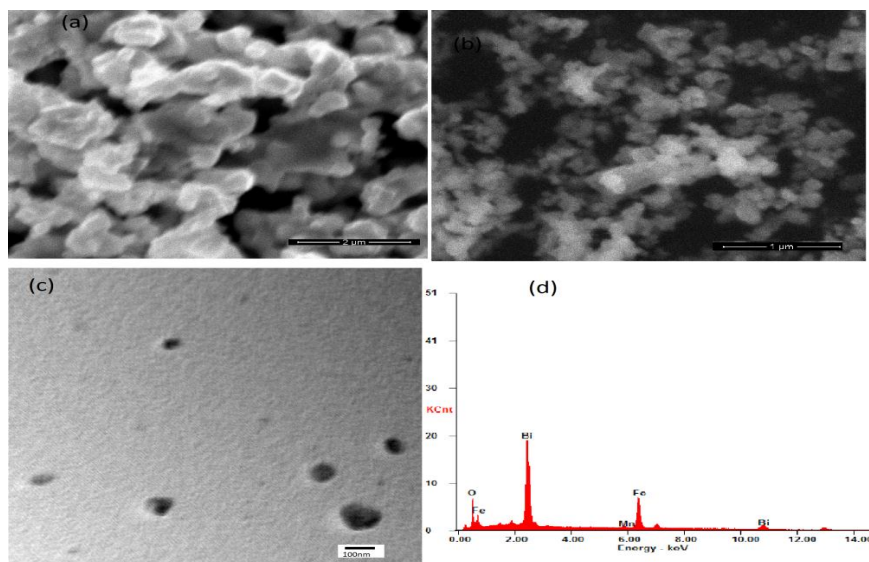


Fig.3. SEM images of (a) pure BFO (b) 5% Mn doped BFO (c) TEM image of 5% Mn doped BFO and (d) EDAX spectra of 5% Mn doped BFO.

It can be noted from SEM images that 5% Mn doped BFO sample has improved surface morphology in contrary to pure BFO which exhibits porous network. Furthermore, there is a significant reduction of particles size with Mn doping. Figure 3(c) shows the tunneling electron microscopy (TEM) image of 5% Mn doped sample. The average particle size from TEM image for 5% sample is around 66nm which is in consistent with that calculated from XRD result.

Dielectric constant and dielectric loss as a function of frequency are shown in Figures 4(a) and 4(b). All samples show similar behavior with increasing frequency. At low frequency, dielectric constant and dielectric loss decrease as the frequency increases up to 200 kHz and thereafter shows a frequency independent behavior. This behavior at low frequency has been explained on the basis of dielectric relaxation phenomena where different dipoles at low frequency are able to follow the frequency of the applied field.

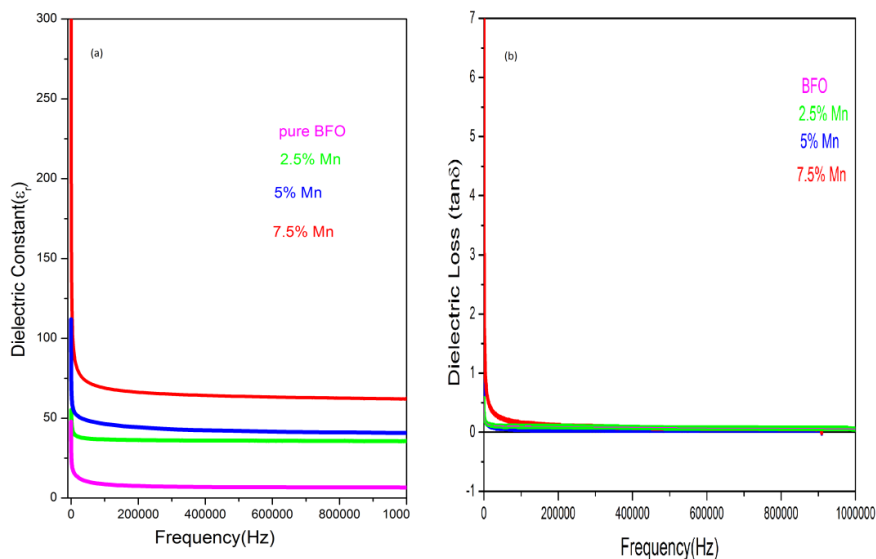


Fig.4 (a) Variation of dielectric constant (ϵ') and (b) dielectric loss ($\tan\delta$) with frequency for $\text{BiFe}_{1-x}\text{Mn}_x\text{O}_3$ nanoparticles at room temperature.

Dielectric constant increases significantly from 19 for BFO to 66 for 7.5% composition while the dielectric loss remains below 0.016 for all samples beyond 200 kHz. The enhancement in dielectric constant with increasing Mn contents may be attributed to the increased interfacial polarization which arises due to large volume fraction of grain boundary as a consequence of decrease in grain sizes [16, 28].

Figures 5(a) and 5(b) show the variation of dielectric constant and dielectric loss as a function of temperature. A temperature variation of permittivity and dielectric loss further indicates the improved dielectric characteristics for 5% Mn doped sample. A small dielectric anomaly is observed for 2.5% sample at 210⁰C which almost disappear for 5% sample and shows a stable behavior up to a temperature of 500⁰C. The dielectric loss increases monotonically with varying temperature up to 300⁰C and thereafter shows a sharp rise due to increased thermal conductivity which is consistent with the earlier reported result [29].

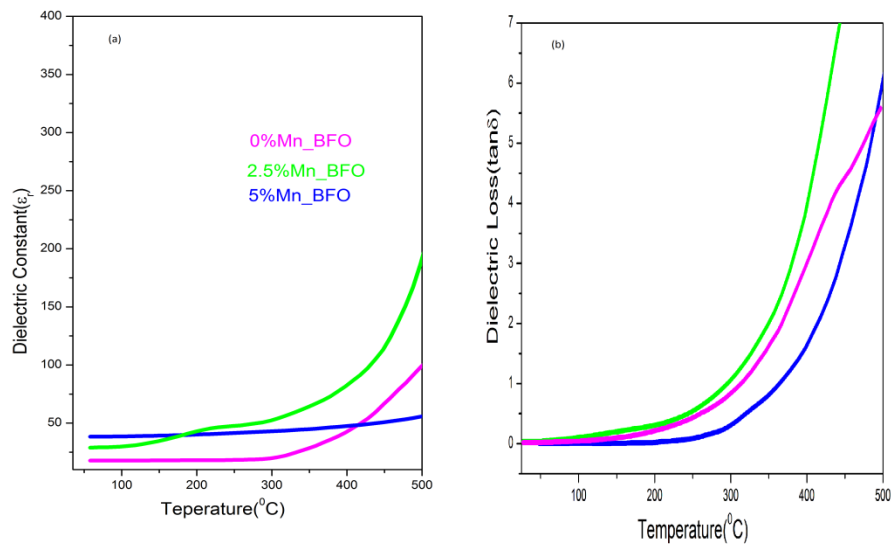


Fig.5 (a) Temperature dependence of dielectric constant (ϵ) and (b) dielectric loss ($\tan\delta$) for $\text{BiFe}_{1-x}\text{Mn}_x\text{O}_3$ nanoparticles at 100 kHz.

The polarization-electric field (P-E) hysteresis loop measured at frequency of 50 Hz at room temperature has been used to study the effect of Mn doping on the ferroelectric properties of BFO nanoparticles. As shown in figure 6, a well saturated hysteresis loop is not possible to observe in any samples due to the presence of high leakage current; however there is an enhancement in the remnant polarization with maximum value of $1.8 \mu\text{C}/\text{cm}^2$ at an applied field of $80\text{kV}/\text{cm}$ for 5% Mn-doped BFO sample. The sample with 7.5% composition shows loopy hysteresis loop even at low applied field due to its highly conductive nature.

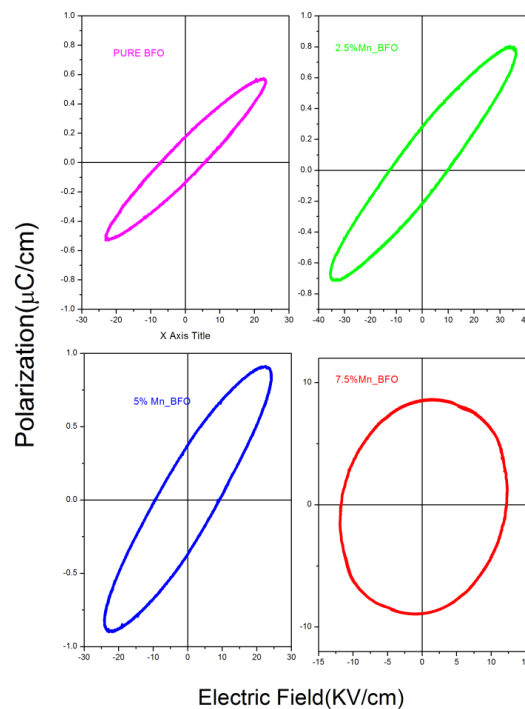


Fig.6. Polarisation-Electric field (P-E) hysteresis loops of $\text{BiFe}_{1-x}\text{Mn}_x\text{O}_3$ nanoparticles at room temperature.

The maximum value of polarization as observed in our samples is small compared with Mn doped BFO thin film and ceramic [30, 31].

The magnetic properties of Mn doped BFO nanoparticles have been studied from M-H hysteresis loops with maximum applied field of 20 kOe. Figure 7 shows the M-H curves for pure and Mn doped BFO samples measured at room temperature. The pure BFO nanoparticles show a small spontaneous magnetization in contrary to antiferromagnetic bulk BFO. This result is in consistent with other report and may be attributed to the fact that the spiral spin structure is partially destroyed in BFO nanoparticles [32-34].

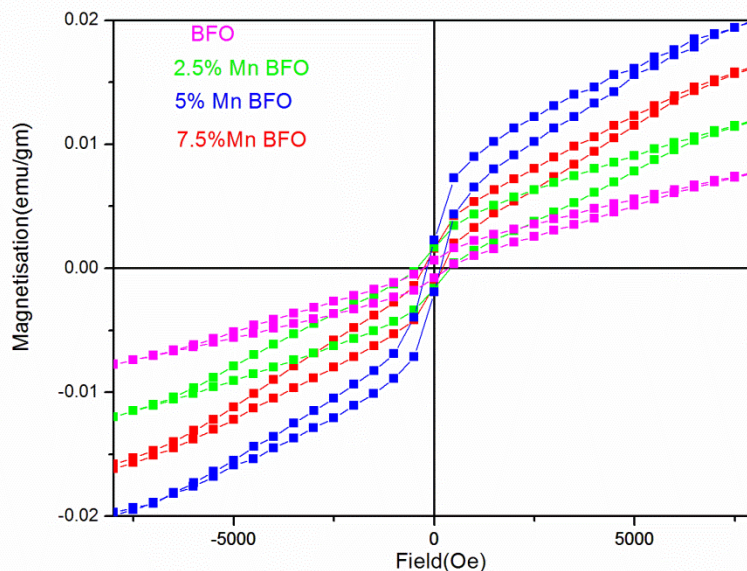


Fig.7. Magnetization vs field (M-H) curves for $\text{BiFe}_{1-x}\text{Mn}_x\text{O}_3$ nanoparticles measured at room temperature.

Saturation magnetization increases slightly with Mn doping and reaches a maximum value of 0.02 emu/g for 5% composition. An enhanced magnetic properties in Mn doped samples (up to 5%) might be either due to effective suppression of spiral spin structure with Mn doping as a consequence of decrease in grain size or breakdown of balance between the antiparallel sublattice magnetization of Fe^{3+} due to metal ions substitution with different valence [35-37].

Further experiments like XPS, Mossbauer spectra, Raman spectra and capacitance-voltage (C-V) measurements can help in identifying the oxidation state of Fe, and ferroelectric behavior which are matter of further investigation.

IV. CONCLUSIONS

$\text{BiFe}_{1-x}\text{Mn}_x\text{O}_3$ ($x = 0.0-7.5\%$) nanoparticles were successfully synthesized by tartaric acid assisted sol-gel method followed by rapid cooling process. XRD patterns indicate secondary phases in pure BiFeO_3 (BFO) which get suppressed with Mn concentration up to 5%. The observation of absorption peaks at 559 cm^{-1} and 432 cm^{-1} in FTIR spectra confirms the formation perovskite structure. The Mn substitution at B-site of BFO improves the particles surface morphology and reduces the average particles size to around 65nm. Dielectric constant increases from 19 for pure BFO to 46 for 5% composition while their loss tangent decreases from 0.2 to 0.016, respectively. A small dielectric relaxation peak is observed for 2.5% composition which disappears for 5% due to reduction of charged defects such as oxygen ion vacancies. The ferroelectric behavior improves with Mn-doping with a maximum remnant polarization value of $1.8\mu\text{C}/\text{cm}^2$ at a maximum applied field of $80\text{ kV}/\text{cm}$. Enhanced magnetic property is observed for 5% composition having maximum value of saturation magnetization of $0.20\text{ emu}/\text{gm}$. Although this value of magnetization obtained is very small, but it can be quite beneficial for some specific applications at room temperature such as spintronic and spin

valve. This study reveals that the Mn doping up to 5% improves the characteristic properties of BFO nanoparticles prepared by rapid cooling process.

ACKNOWLEDGEMENT

The authors wish to acknowledge University Grant Commission- India, for financial assistance under Junior Research Fellowship (JRF) scheme. Thanks are also due Defence Research and Development Organization, India for providing Dielectric measurements Facilities.

REFERENCES

- [1]. M. Fiebig, *J. Phys. D: Appl. Phys.*, 38 (2005) R123.
- [2]. K. F. Wang, J. M. Liu, Z. F. Ren, *Adv. Phys.*, 583(2009) 21.
- [3]. C. W. Nan, M. I. Bichurin, S. X. Dong, D. Viehland, G. Srinivasan, *J. Appl. Phys.*, 103 (2008) 031101.
- [4]. G. A. Smolenskii, I. E. Chupis, *SoV, Phys. Usp.* 25 (1982) 475-493.
- [5]. K. F. Wang, J. M. Liu, Z. F. Ren, *Adv. Phys.*, 58 (2009) 321.
- [6]. D. Rajasree, K. G. Gopal, M. Kalyan, *J. Appl. Phys.*, 111 (2012)104115.
- [7]. K. G. Yang, Y. L. Zhang, S. H. Yang, B. Wang, *J. Appl. Phys.*, 107 (2010) 124109.
- [8]. S. X. Dong, J. Y. Zhai, J. F. Li, D. Viehland, M. I. Bichurin, *Appl. Phys. Lett.*, 89 (2006) 243512.
- [9]. G. A. Smolenskii, I. E. Chupis, *Sov. Phys.—Usp.* 25 (1982) 475.
- [10]. S. K. Singh, H. Ishiwara, *Japan. J. Appl. Phys.*, 44 (2005) L734–6.
- [11]. Y. P. Wang, L. Zhou, M. F. Zhang, X. Y. Chen, J. M. Liu, Z. G. Liu, *Appl. Phys. Lett.*, 84 (2004) 1731.
- [12]. H. Uchida, R. Ueno, H. Funakubo, S. Koda, *J. Appl. Phys.*, 100 (2006) 014106.
- [13]. F. Z. Huang, X. M. Lu, W. W. Lin, X. M. Wu, Y. Kan, J. S. Zhu, *Appl. Phys. Lett.* 89 (2006) 242914.
- [14]. B. F. Yu, M. Y. Li, Z. Q. Hu, D. Y. Guo, X. Z. Zhao, S. X. Dong *Appl. Phys. Lett.*, 93 (2008) 182909.
- [15]. I. O. Troyanchuk, O. S. Mantyskaya, A. N. Chobot, N. V. Tereshko, *Phys. Solid State* 51, 2105 (2009).
- [16]. M. Kumar, K. L. Yadav, *Appl. Phys. Lett.* 91 (2007) 242901.
- [17]. X. D. Qi, J. Dho, R. Tomov, M. G. Blamire, J. L. MacManus-Driscoll, *Appl. Phys. Lett.*, 86, (2005) 062903.
- [18]. Wu Jiagang, John Wang. *J. Am. Ceram. Soc.*, 93 [9] 2795–2803.
- [19]. S. K. Singha_ K. Maruyama, H. Ishiwara. *Appl. Phys. Lett* 91, (2007) 112913.
- [20]. Tae-Jin, Park, C. Georgia. Papaefthymiou, J. Arthur. L. Viescas, R. Arnold. Moodenbaugh, S. Stanislaus. *nano letter*, (2007) Vol, 7 No,3.
- [21]. S. Basu, M. Hossain. D. Chakravorty, M. Pal, *Current Applied P*, 11(2011) 976-980.
- [22]. JCPDS Card No. 86-1518.
- [23]. J. R. Teague, R. Gerson, W. J. James, *Solid State Commun*, 8 (1970) 1073.
- [24]. R. K. Mishra, D. K. Pradhan, R. N. P. Chaudhary, A. Banerjee, *J. Phys.:*
- [25]. *Condens. Matter*, 20 (2008) 045218.
- [26]. G. V. Subba Rao, C. N. R. Rao, *Appl. Spectrosc.* 24 (1970) 436.
- [27]. C. Chen, J. Cheng, S. Yu, L. Che, Z. Meng *J. Cryst. Growth* 291(2006) 135 Vol. 7, No. 3.
- [28]. O. Yamaguchi, A. Narai, T. Komatsu, K. Shimizu, *J. Am. Ceram. Soc.* 69, 256–257 (1986) 766-772.
- [29]. A. K. Jonscher, F. Meca, H. M. Millany, *J. Phys. C: Solid State Phys.* 12 (1979) L29329.
- [30]. M. Polomska, W. Kaczmerk, Pajak, *Z Phys. Status Solidi a* 23 (1974) 567.
- [31]. M. Kumar, K. L. Yadav, *Appl. Phys. Lett.* 91 (2007) 112911.
- [32]. M. Kumar, K. L. Yadav. *Appl. Phys. Lett.*, 91 (2007) 242901.
- [33]. R. Mazumder, P. Sujatha Devi, D. Bhattacharya, P. Choudhury, A. Sen, M. Raja, *Appl. Phys. Lett.* 91 (2007) 062510.
- [34]. J. Wang, A. Scholl, H. Zheng, S. B. Ogale, L. Viehland, D. G. Schlom, N. A. Spaldin, K. M. Rabe, M. Wuttig, L. Mohaddes, J. Neaton, U. Waghmare, T. Zhao, R. Ramesh, *Science*, 307 (2005) 1203b.
- [35]. T. Kanai, S. I. Ohkoshi, K. Hashimoto, *J. Phys. Chem. Solids*, 64 (2003) 391.
- [36]. A. Sundaresan, R. Bhargavi, N. Rangarajan, U. Siddesh, C. N. R. Rao, *Phys. Rev. B* 74 (2006) 161306.
- [37]. D. Kothari, V. R. Reddy, A. Gupta, D. M. Phase, N. Lakshmi, S. K. Deshpande. A. M. Awasthi, *J. Phys.:* *Condens. Matter* 19 (2007) 136202.
- [38]. K. S. Nalwa, A. Garg, *J. Appl. Phys.*, 103 (2008) 044101.

AUTHORS BIOGRAPHY

Ghanshyam Arya did his M.Sc. and M.phil. from himachal Pradesh university. He has been doing his research work for last two years on multiferroic materials. His research work is financed by UGC, India under JRF scheme. He has attended many national and international conferences.



Ashwani Kumar did his M.Sc. and M.phil. from himachal Pradesh university. He is actively doing his research work on composites multiferroics. He has attended many national workshop, seminar and international conferences and has good exposure of his research field.



Mast Ram joined the govt. degree college, arki, himachal Pradesh, india in 1998 and has been actively doing his research work in himachal Pradesh university for last four years. He has numerous publications to his credit and is currently working on diluted magnetic semiconductor.



N.S. Negi joined the Himachal Pradesh University, Shimla in October 1997 after two years as a faculty member at Department of Physics, Govt. Degree College Seema, India. He received his PhD degree from the Himachal Pradesh University Shimla. He has extensive experience in deposition of ferroelectric & ferrite thin films. He currently works on ferroelectric & multiferroic thin films, high k materials, diluted magnetic semiconductors & pyrophoric materials. He has published over 40 papers in international journals. Currently he is a Professor & Head, Department of Physics. H.P. University, Shimla

